UDC 669.162.12:622
DOI 10.17073/0368-0797-2023-5-529-537

Original article
Оригинальная статья

Development of equipment and technology for pelletizing iron ore charge in production of pellets

V. M. Pavlovets

Siberian State Industrial University (42 Kirova Str., Novokuznetsk, Kemerovo Region – Kuzbass 654007, Russian Federation)

pawlowets.victor@yandex.ru

Abstract. New possibilities of pelletizing process in pellet production can improve the production performance. The principles of induced nucleation in the pelletizing technique expand its technological capabilities. The technical indicators of the new pellet production technology and the physical parameters of wet pellets make it possible to increase the metallurgical properties of agglomerated raw materials. The presented technical diagrams reflect the production capabilities of induced nucleation in the processes of forming a sprayed layer (SL) of the charge and its division by various technical devices. The design features and technological modes of the developed technical schemes are implemented on a typical disc pelletizer. Experimental data obtained during implementation of the developed technological schemes make it possible to change the relative values of strength, mass and moisture content of the pellets during pelletizing of the iron ore charge. These parameters can be adjusted during loading of charge, its spraying onto the charge shell of the pelletizer, dividing the sprayed layer of the charge into nuclei and further pelletizing of the nuclei to form a pellet shell. An assessment of these technological schemes led to selection of the most effective solutions based on thermal power spraying of wet charge, taking into account its adhesion, material consumption and complexity of the equipment design. For practical use, we recommend a combined technological scheme for the production of pellets using the induced nucleation technology on the basis of SL formation of a single air-charge jet (ACJ) containing strengthening additives, on a pre-profiled skull and dividing the SL into nuclei by a conical drum equipped with a metal string. At the end of the technological cycle of pellet production, increased porosity with a high proportion of open pores is formed in the central embryonic part of the pellets. The pellets have a low moisture content ($\Theta_W = 0.97$) and a favorable pore structure. In the forecast, they require less energy consumption for their subsequent heat treatment. The technology makes it possible to produce pellets with the required and maximum strength ($\Theta_П \geq 1.0$) 12 – 16 mm in size with higher productivity ($\Theta_М = 0.68$). In the course of experiments, it was found that the technology of preliminary nucleation has high reliability and versatility, and it can be easily introduced into the existing production.

Keywords: iron ore raw materials, equipment and technology of pelletizing, agglomerated metallurgical raw materials, iron ore pellets, thermal power spraying of wet charge, induced nucleation

For citation: Pavlovets V.M. Development of equipment and technology for pelletizing iron ore charge in production of pellets. *Izvestiya. Ferrous Metallurgy*. 2023;66(5):529–537. https://doi.org/10.17073/0368-0797-2023-5-529-537

Особенности развития техники и технологии окомкования железорудной шихты в производстве окатышей

В. М. Павловец

Сибирский государственный индустриальный университет (Россия, 654007, Кемеровская обл. – Кузбасс, Новокузнецк, ул. Кирова, 42)

pawlowets.victor@yandex.ru

Аннотация. Новые возможности процесса окомкования в производстве окатышей позволяют улучшить производственные показатели. Принципы принудительного зародышеобразования в технике окомкования расширяют его технологические возможности. Технические показатели новой технологии производства окатышей и физические параметры влажных окатышей позволяют повысить металлургические свойства окускованного сырья. Представленные технические схемы отражают производственные возможности принудительного зародышеобразования в процессах формирования напыленного слоя (НС) шихты и его деления различными техническими устройствами. Конструктивные особенности и технологические режимы разработанных технических схем реализованы на типичном тарельчатом окомкователе. Опытные данные, полученные при реализации разработанных технологических схем, позволяют изменять относительные величины прочности, массы и влажности окатышей в ходе окомкования железорудной шихты. Эти параметры можно регулировать в ходе загрузки шихты, ее напыления на шихтовый гарнисаж окомкователя, деления напыленного слоя шихты на зародыши и доокомкования зародышей с формированием оболочки окатышей. Оценка указанных технологических схем привела к выбору наиболее эффективных решений, основанных на теплосиловом напылении влажной шихты с учетом процесса ее налипания, материалоемкости и сложности конструктивного оформления оборудования. Для практического использования рекомендована комбинированная технологическая схема

получения окатышей по технологии принудительного зародышеобразования на основе формирования НС одиночной воздушношихтовой струей, содержащей упрочняющие добавки, на предварительно профилированный гарнисаж и деления НС на зародыши коническим барабаном, снабженным металлической струной. В конце технологического цикла производства окатышей в центральной зародышевой части окатышей формируется повышенная пористость с высокой долей открытых пор. Окатыши обладают пониженной влажностью ($\Theta_W = 0{,}97$) и благоприятной поровой структурой. В прогнозе они требуют меньших энергозатрат на их последующую термообработку. Технология позволяет выпускать окатыши необходимой и максимальной прочности размером 12 – 16 мм с более высокой производительностью. В ходе экспериментов установлено, что технология предварительного зародышеобразования обладает высокой надежностью и универсальностью, легко внедряется в действующее производство.

Ключевые слова: железорудное сырье, техника и технология окомкования, окускованное металлургическое сырье, железорудные окатыши, теплосиловое напыление влажной шихты, принудительное зародышеобразование

Для цитирования: Павловец В.М. Особенности развития техники и технологии окомкования железорудной шихты в производстве окатышей. *Известия вузов. Черная металлургия*. 2023;66(5):529–537. https://doi.org/10.17073/0368-0797-2023-5-529-537

Introduction

The process of pelletizing an iron ore charge in the production of pellets represents the initial phase of agglomerating raw materials derived from iron ore. This process facilitates the formation of a wet bulk mass, its primary structuring, and subsequent hardening [1; 2]. The primary objective of pelletization is to create round-shaped pellets possessing maximum possible strength, allowing them to withstand transportation and endure thermal operations without softening. The wet charge forming process in pellet production initiates with nucleation and culminates in the final pelletizing of nuclei. In traditional pellet production technology, impacting the nucleation process using existing technical means without involving auxiliary physical fields proves challenging [3]. However, a recent proposal aims to enhance the functionality of the pelletizing section by employing thermal power spraying of the wet charge onto the pelletizer skull. This method endows it with additional shape-generating and structure-forming functionalities during pellet production [4; 5]. Known as the technology of induced nucleation by spraying and final pelletizing (NSF) of nuclei, it significantly transforms the processes of nucleation and pelletization of the iron ore charge. This technology offers a diverse array of tools to influence pellet structural properties and the parameters of pelletizer production [4 – 6]. According to this technology, the initial stage of raw pellets production involves the formation of a dense sprayed layer (SL) of the charge using an air-charge jet (ACJ) within the idle zone of the rotating disc pelletizer. To create an embryonic mass, the SL within the same pelletizer zone is mechanically divided into solid nuclei, having shapes akin to spherocubes or spheroparallelepipeds. During the subsequent forming stage within the pelletizer's working zone containing lumpy materials, the corners and faces of these nuclei are crumpled to form a round shape. Simultaneously, the nuclei undergo final pelletizing while mixed with moistened charge in a rolling mode, thereby forming the pellet shell [6 – 8]. The central part of two-layer pellets exhibits lower moisture content and is characterized by higher porosity, featuring an increased proportion of open pores. The low moisture content of such raw pellets, coupled with this porosity pattern, mitigates crack formation and significantly reduces the temperature of shock fracture during drying [4; 5]. Consequently, the likelihood of a decrease in strength of annealed pellets during subsequent metallurgical treatment diminishes. Even after undergoing intense firing, the structure of pellets maintains an augmented number of permeable pores open to reducing gases [5]. This specific pellet structure minimizes diffusion limitations during subsequent reduction processes and enhances the reactivity of agglomerated raw materials. Similar structural properties of pellets can also be achieved by utilizing pore-forming biomass [7; 8] or complementary technologies [9 – 11]. Figs. 1 and 2 depict the schematic representation of NSF technology and the macrostructure of the materials involved in wet charge forming. Implementing the production scheme can be readily accomplished within existing sites possessing available manufacturing areas and technical capabilities. The NSF technology has laid the groundwork for various technical solutions [4; 5] that facilitate the control of nucleation processes, pellet formation, and their physical properties. By analyzing the operational processes of nuclei and pellets, one can formulate the general principles governing nucleation and structurization of the lumpy mass within this technology.

The primary aim of this paper is to analyze the technical solutions directed towards equipment and technology development for pelletizing iron ore charge during pellet production based on induced nucleation.

Materials and methods

Fig. 3 display technical diagrams of devices used in pellet production, showcasing different methods of forming the dense SL by spraying the wet charge onto the skull. Meanwhile, Fig. 4 present schematic representations of the diverse methods employed to divide the SL into nuclei within these devices. It's important to note that the author has secured patents from the Russian Federation for the depicted technical schemes (Figs. 3, 4). For the implementation of the pellet production technical schemes, the laboratory semi-industrial disc pelletizer served as the foundational apparatus

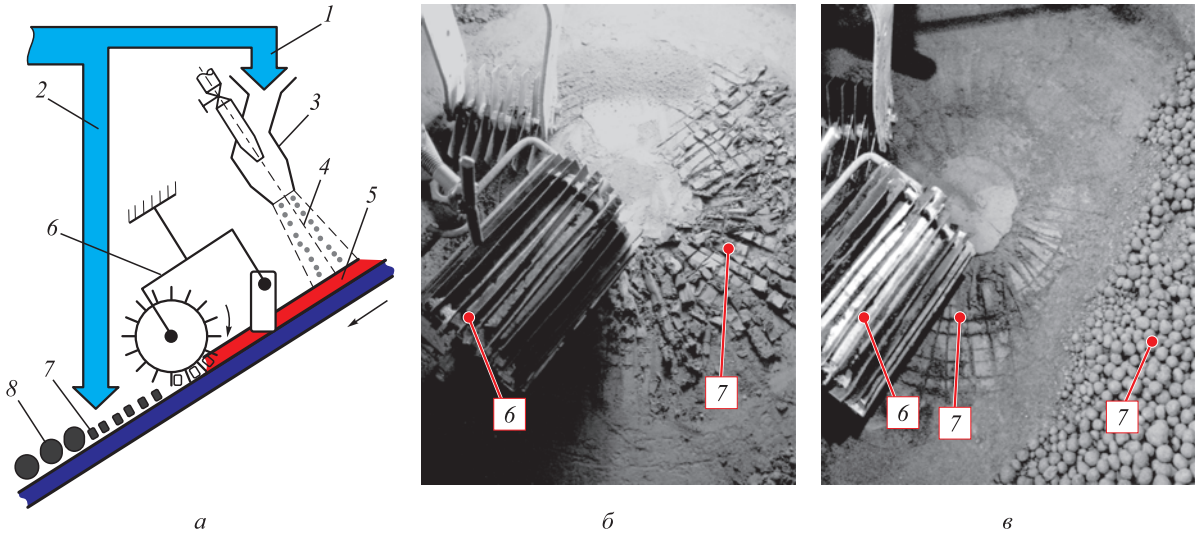

а *б* *в*

Fig. 1. Scheme of wet charge forming into nuclei and pellets (*a*) and appearance of experimental installation based on a disk pelletizer for producing pellets using the NSF technology (nucleation by spraying and final pelletizing of nuclei – *b*, *c*):
1 – charge flow for nucleation; *2* – charge flow for the final pelleting of nucleus; *3* – jet unit; *4* – air-charge jet; *5* – sprayed charge layer; *6* – SL divider, consisting of longitudinal (lamellar knives) and transverse (rotating drum with edges) dividers; *7* – nucleus; *8* – pellets

Рис. 1. Схема формообразования влажной шихты в зародыши и окатыши (*а*) и внешний вид экспериментальной установки на основе тарельчатого окомкователя для получения окатышей по технологии ЗНД (*b*, *c*):
1 – поток шихты для зародышеобразования; *2* – тоже для доокомкования зародышей; *3* – струйный аппарат; *4* – воздушношихтовая струя; *5* – напыленный слой шихты; *6* – делитель НС, состоящий из продольного (пластинчатые ножи) и поперечного (вращающийся барабан с ребрами) делителей; *7* – зародыши; *8* – окатыши

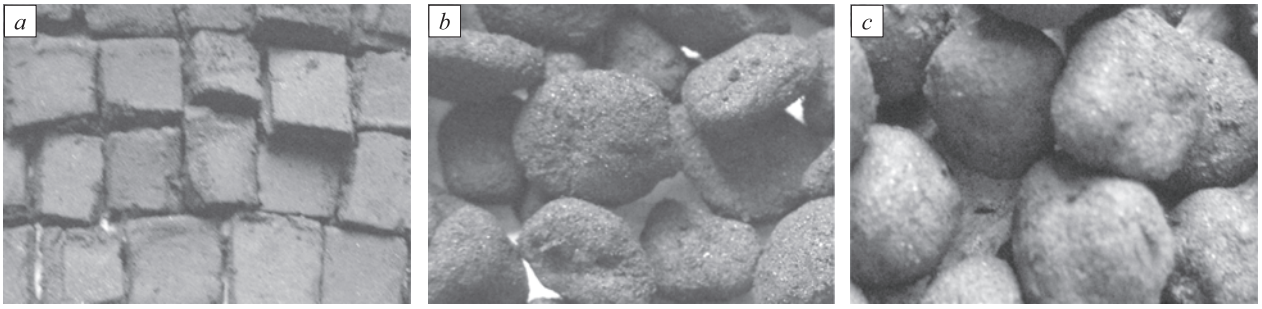

Fig. 2. Appearance of charge materials and sequence of pellets formation from nuclei using NSF technology:
a – fragment of SL divided into nuclei; *b* – nucleus 60 s after final pelletizing; *c* – nucleus 300 s after final pelletizing

Рис. 2. Внешний вид шихтовых материалов и последовательность формирования окатышей из зародышей по технологии ЗНД:
а – фрагмент НС, разделенного на зародыши; *b* и *c* – зародыши через 60 и 300 с после доокомкования соответственно

(diameter 0.62 m, disc inclination angle $\gamma = 45°$, number of revolutions $n = 12$ rpm). The pelletizer is equipped with a jet unit (JU) (diameter $d_{JU} = 0.02$ m, charge flow rate $G_{sh} = 0.03 – 0.04$ kg/s, pressure $P_a = 0.2$ MPa, compressed air flow rate $V_a = 0.6$ m^3/min) and variously designed devices for dividing the SL into nuclei. To implement the multi-jet technical schemes initially, three JUs, each with a diameter of 0.02 m, were utilized, all operating under identical initial conditions and maintaining the same charge flow rate. The wet charge employed in this process consisted of iron-ore concentrate sourced from the Tei deposit ($d_h = 0.068$ mm) and 1 % bentonite. A 5-kg charge was sprayed over a period of 60 s onto the 30 mm thick charge skull (CS) ($\rho_{CS} = 2230$ kg/m^3, $W_{CS} = 8.14$ %) present in the idle zone of the disc, positioned at $\Theta_L = 25$ ($\Theta_L = L/d_{JU}$ – dimensionless distance, $L = 0.5$ m). For the final pelletizing of nuclei and the formation of standard pellets, an additional 5 kg of wet charge were introduced into the pelletizer's working zone. Average strength and moisture content measurements were conducted for all formed materials. The dimensions of the SL were measured (diameter d_{SL}, m and SL height on its axis h_t, m). Subsequently, the embryonic mass and the array of pellets were sieved. The sampling methodology is detailed in [4; 5].

For the technical schemes implementing of various methods of SL formation (Fig. 3), the spraying coefficient C_{SL}, %, was calculated as follows:

$$C_{SL} = \frac{M_{sh} - M_m}{M_{sh}},$$

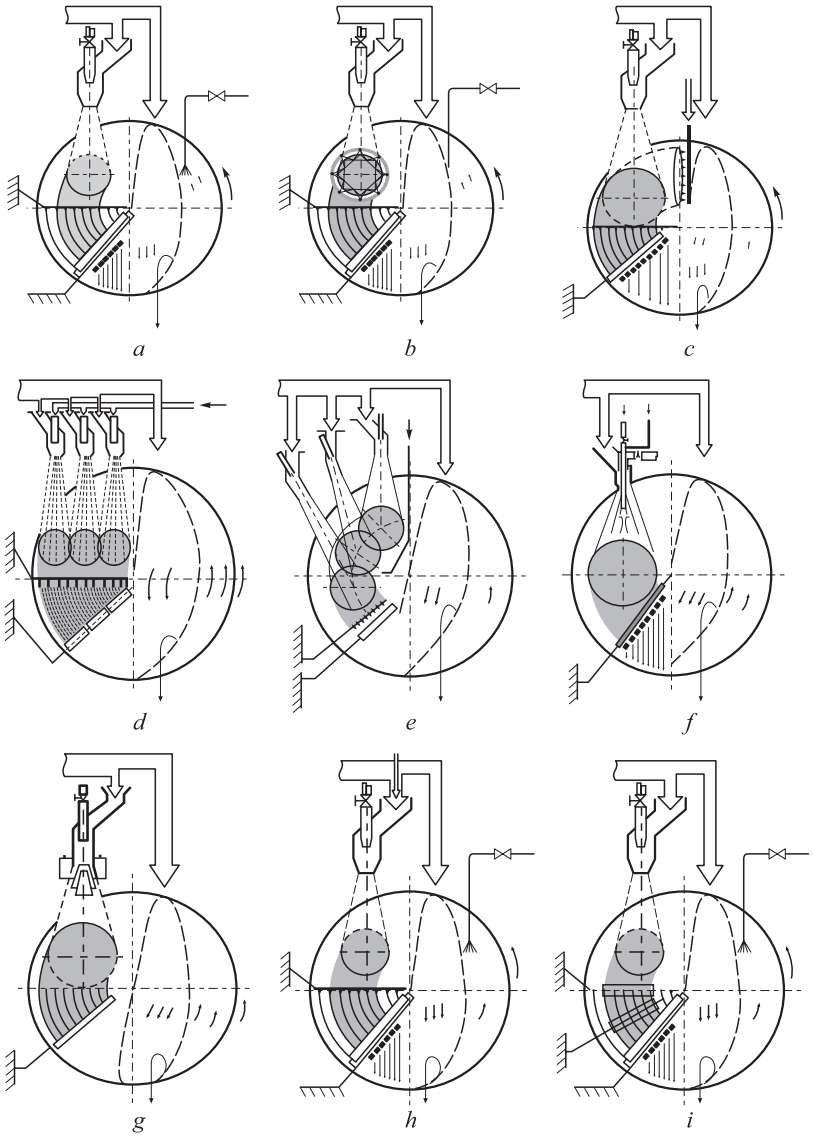

Fig. 3. Technical schemes of SL formation on pelletizer skull:
a – one ACJ; *b* – the same with moistening of the deposition zone; *c* – moistening of the charge skull (CS); *d* – several ACJ with superposition of SL along the radius; *e* – the same with superposition of SL along an arc; *f* – one ACJ with auxiliary air flow; *g* – one ACJ with deflecting nozzles on the path of ACJ; *h* – one ACJ with hardening additives in the charge; *i* – additional compaction of SL with drums

Рис. 3. Технические схемы формирования НС на гарнисаже окомкователя:
a – одной ВШС; *b* – тоже с увлажнением зоны напыления; *c* – увлажнение ШГ; *d* – несколькими ВШС с наложением НС по радиусу; *e* – тоже с наложением НС по дуге; *f* – одной ВШС с вспомогательным потоком воздуха; *g* – одной ВШС с отклоняющими насадками на пути ВШС; *h* – одной ВШС с упрочняющими добавками в шихте; *i* – дополнительное уплотнение НС барабанами

where M_{sh} is the mass of the deposited charge, kg; M_m is the mass of the charge remaining after SL formation, kg.

For the technical schemes implementing various methods of SL division into nuclei (Fig. 4), the fractional composition of the embryonic mass and the nucleation coefficient C_{nucl}, %, were determined using the following formula:

$$C_{nucl} = \frac{M_{nucl}}{M_{sh}} = \frac{M_{sh} - M_m - M_n}{M_{sh}},$$

where M_{nucl} is the mass of nuclei ranging from 2 to 10 mm in size, kg; M_n is the mass of nuclei fines smaller than 2 mm in size, kg.

Multiple experiments were conducted for each technical scheme, enabling the acquisition of average values for the parameters being analyzed. In order to provide a comprehensive assessment of the NSF technology's efficiency and the properties of the SL, nuclei, and pellets, certain experimental outcomes were presented in dimensionless form, as discussed in [4; 5]. The relative strength of the molded materials, denoted as Θ_S, was determined using the equation

$$\Theta_S = \frac{S_{av}}{S_p},$$

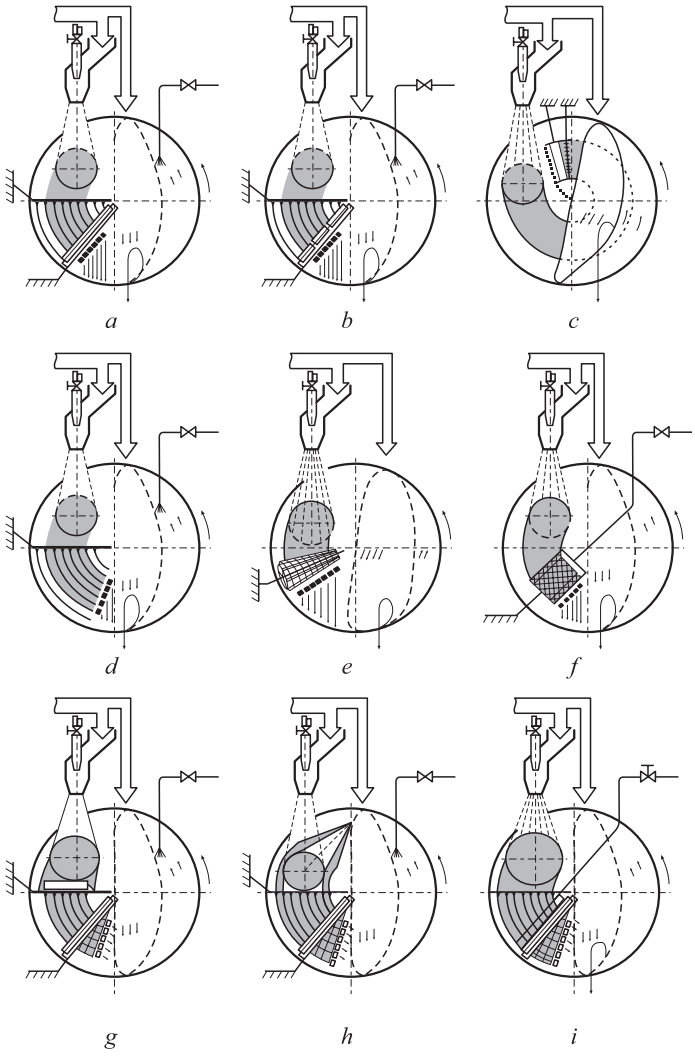

Fig. 4. Technical schemes of charge SL division into nuclei on pelletizer skull with:
a – longitudinal plate knives and drum with transverse ribs; *b* – the same with composite rotating drums; *c* – division of SL by longitudinal plate knives and rotating drum with transverse ribs at outlet from lumpy materials layer; *d* – plow dividers; *e* – conical drum equipped with metal strings; *f* – drum equipped with ribs with semicircular cells; *g* – SL profiling in width and height; *h* – CS profiling; *i* – drum with transverse ribs and system of rods

Рис. 4. Технические схемы деления напыленного слоя шихты на зародыши на гарнисаже окомкователя:
a – продольными пластинчатыми ножами и барабаном с поперечными ребрами; *b* – тоже с составными вращающимися барабанами; *c* – деление НС продольными пластинчатыми ножами и вращающимся барабаном с поперечными ребрами на выходе из слоя комкуемых материалов; *d* – плужковыми делителями; *e* – коническим барабаном, снабженным металлическими струнами; *f* – барабаном, снабженным ребрами с полукруглыми ячейками; *g* – с профилированием НС по ширине и высоте; *h* – с профилированием ШГ; *i* – барабаном с поперечными ребрами и системой стержней

where S_{av} is the average strength of samples from SL, nuclei and pellets, kPa, S_p is the average strength of pellets, 12 – 16 mm in size, kPa, and S_p = 280 kPa.

The relative mass of molded materials (SL, nuclei, and pellets) Θ_M was calculated using the formula

$$\Theta_M = \frac{M_m}{M_t},$$

where M_m is the average mass of molded materials (SL, nuclei, and pellets), kg, M_t is the total mass of the charge used in pellet production, inclusive of the charge fed for the final pelletizing of nuclei in the pelletizer's working zone, kg, M_t = 10 kg.

The relative moisture content of the molded materials Θ_W was evaluated using the equation

$$\Theta_W = \frac{W_{av}}{W_{sh}},$$

where W_{av} is the average moisture content of the samples from SL, nuclei, and pellets, %, W_{sh} is the moisture content of the deposited charge, %, set at W_{sh} = 8.2 %.

The relative duration of the processes involving charge loading, depositing, SL division, and final pelletizing of nuclei, represented as Θ_τ, was calculated using the equation

$$\Theta_\tau = \frac{\tau_i}{\tau_p},$$

where τ_i is the duration encompassing charge loading, depositing, SL division, and final pelletizing of nuclei, s. The time periods for depositing, SL division, and final pelletizing of nuclei were to 15, 5 and 300 s, respectively. Meanwhile τ_p represent the total duration of pelletization, set at $\tau_p = 380$ s.

To determine the characteristics of SL (C_{SL}, Θ_M, Θ_S, Θ_W), formed in various ways (Fig. 3), the pelletizer was operated without dividers throughout the entire spraying period. In order to conduct a comparative analysis of the performance of these diverse technical schemes, we utilized the fundamental scheme (Fig. 3, *a*). This scheme relied on a single JU operation, spraying the wet charge onto an unprepared CS. It is noteworthy that most industrial depositing technologies entail numerous performance requirements concerning spraying devices and techniques, as indicated in [12 – 15].

To calculate the parameters of the embryonic mass (fractional composition, C_{nucl}, Θ_M, Θ_S, Θ_W) acquired via various methods of SL division into nuclei (Fig. 4), the SL divider was utilized on the pelletizer subsequent to SL formation. For a comparative assessment of these technical schemes, we utilized the fundamental scheme (Figs. 1 and 3, *a*), which was additionally equipped with a divider featuring longitudinal (lamellar knives) and transverse (rotating drum with edges) dividers coated with bakelite varnish to prevent charge adhesion (Fig. 4, *a*).

Results and discussion

Fig. 5 illustrates the typical changes in parameters Θ_M, Θ_S, Θ_W during the process of charge formation, which includes charge deposition, SL formation, and its subsequent division into nuclei, followed by pelletization.

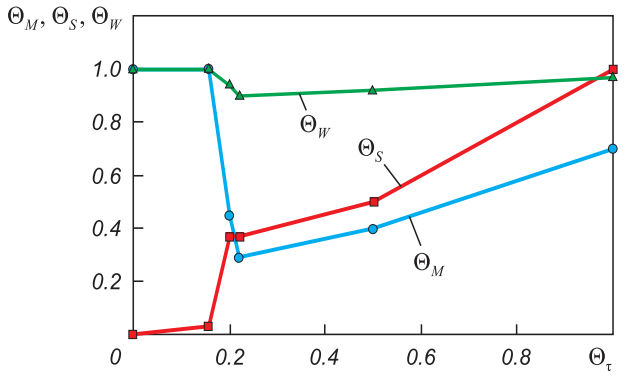

Fig. 5. Kinetics of changes in relative strength Θ_S, mass Θ_M and moisture content Θ_W of materials during charge forming and pellets formation

Рис. 5. Кинетика изменения относительной прочности Θ_S, массы Θ_M и влажности Θ_W материалов в процессе формообразования шихты и формирования окатышей

These trends were observed in the basic spraying scheme (Figs. 3, *a* and 4, *a*). The experimental results are comprehensively presented in Tables 1 and 2. The dependencies obtained from these experiments, as depicted in Fig. 5, allow for the generalization of research outcomes and the identification of potential constraints within the NSF technology. Across all technical schemes detailed in Tables 1 and 2, a consistent observation is the rapid formation of the wet charge, showcasing an average nuclei mass growth rate exceeding 3.0 g/s. This rapid growth is accompanied by an increase in strength ($\Theta_S > 0.39$) and relatively minor mass loss of the formed materials during the stages of charge deposition (up to $\Theta_M = 0.44$) and SL division (up to $\Theta_M = 0.29$) into nuclei (Fig. 5). It has been noted that enhancing the strength of the SL during charge deposition ($\Theta_S > 0.8 – 0.9$) [4; 5] brings it closer to that of the whole pellet. However, this particular regime results in decreased porosity and a reduction in the proportion of open pores in the embryonic part of the pellet, which contradicts the fundamental structurization principles of the NSF technology. The slight increase in nuclei strength during SL division can be attributed to the mechanical compaction of the wet mass facilitated by dividers or supplementary devices. During the final pelletizing phase of the nuclei, both the mass and strength of the pellets increase as the shell forms in the rolling mode. The dehydration process of the SL is closely associated with barodiffusive moisture transfer facilitated by the ACJ, into which the SL and embryonic mass come into contact during the spraying process. The final pelletizing phase of nuclei is accompanied by the growth of parameters Θ_M, Θ_S, Θ_W, includes several stages and extends over a longer dura-

Table 1

Indicators of technical schemes that implement various methods of SL formation

Таблица 1. **Показатели технических схем, реализующих различные способы формирования НС**

The scheme is presented in Fig. 3	Indicators					
	C_{SL}	d_{SL} / d_{JU}	d_{SL} / h_t	Θ_M	Θ_S	Θ_W
a	0.88	10.5	20.5	0.44	0.39	0.96
b	0.95	11.5	21.5	0.46	0.41	0.99
c	0.92	11.5	21.5	0.46	0.42	0.97
d	0.92	29.0	94.0	0.46	0.40	0.96
e	0.91	11.5	21.5	0.46	0.45	0.94
f	0.88	14.5	59.0	0.43	0.36	0.96
h	0.86	15.0	60.0	0.43	0.35	0.96
h	0.86	10.5	20.5	0.45	0.48	0.96
i	0.88	11.5	23.5	0.44	0.45	0.95

Table 2

Indicators of technical schemes that implement various methods of SL division into nuclei

Таблица 2. **Показатели технических схем, реализующих различные способы деления НС на зародыши**

The scheme is presented in Fig. 4	Indicators								
	nuclei fractional composition, mm					A_{nucl}, mm	C_{nucl}	Θ_M	Θ_S
	0 – 2	2 – 4	4 – 6	6 – 10	>10				
a	34.1	18.8	18.2	28.1	0.8	4.34	0.58	0.29	0.42
b	32.5	18.5	20.2	28.4	0.4	4.21	0.61	0.30	0.42
c	33.2	19.5	20.5	26.2	0.6	4.09	0.61	0.30	0.51
d	43.4	22.6	15.4	10.4	8.2	2.71	0.45	0.22	0.41
e	26.1	18.6	24.6	30.2	0.5	4.51	0.69	0.35	0.43
f	25.4	19.3	25.4	29.9	0	4.49	0.58	0.29	0.42
h	15.2	21.3	30.6	32.9	0	5.67	0.62	0.31	0.42
h	12.3	22.2	31.9	33.6	0	6.22	0.67	0.38	0.42
i	32.1	19.8	20.2	26.1	0.8	4.15	0.58	0.29	0.38

tion (300 s), significantly slowing down both the growth rate of mass (to 0.11 g/s) and strength [4; 5]. During this phase, the moisture content of pellets formed in the final pelletizing stage increases due to excessive moistening of the pellet shell. In the majority of technical schemes employing the NSF technology for final pellet production, the focus is on forming the maximum number of pellets sized between 12 to 16 mm ($\Theta_M > 0.7$). These pellets exhibit an average mass growth rate (more than 0.3 g/s), attain the required strength ($\Theta_S = 1.0$), and demonstrate reduced moisture content in their structure ($\Theta_W < 1$). In the central embryonic part of the pellets, this decrease is even greater ($\Theta_W < 0.95$).

An analysis of the efficiency of the reviewed technical schemes would be prudent. The scheme depicted in Fig. 3, *b*, deviates from the basic one by intensively moistening the deposition zone and the SL surface. This alteration allows for an increase in CSL to 0.95 and augmentation of the SL's geometrical dimensions and parameters Θ_M, Θ_S, Θ_W (Table 1). However, the excessive moistening of the SL to $W_{SL} = 0.99W_{sh}$ and, consequently, the nuclei and resultant pellets, prolongs the subsequent drying duration of pellets during the heat treatment stage. Similarly, the scheme illustrated in Fig. 3, *c*, results in similar SL characteristics by premoistening the charge before spraying, differing from the basic solution. The scheme presented in Fig. 3, *d*, enhances the transverse dimensions and maintains a consistent SL thickness by overlapping boundary zones ($\delta = 1.0 – 0.8$, where δ denotes the dimensionless radius of the SL). These SL zones exhibit high porosity and low strength. A similar effect on the spraying process is detailed in [16 – 20], associating control of the dispersed phase flow rate in the JU with variations in the rotation speed of the sprayed base. The scheme displayed in Fig. 3, *e*, is notably more intricate and diverges from the basic scheme by employing successive charge spraying using three JUs, thereby expanding the longitudinal deposition area. This extended exposure of the ACJ to the SL for approximately three times longer increases the SL strength by around 10 – 15 %. It intensifies moisture removal from the SL, maintaining indicator levels Θ_M, Θ_W closely resembling those of the basic scheme. The scheme shown in Fig. 3, *f*, focuses on improving the uniformity of SL thickness by utilizing a single JU operating alongside auxiliary fan-supplied air along the JU axis. This modification results in larger geometric dimensions of the SL due to the expansion angle of the jet increasing to 30°. However, a drawback of this scheme is the reduced strength properties of the SL due to decreased ACJ pressure. The scheme illustrated in Fig. 3, *g*, involves deflecting mechanical devices positioned in the path of the ACJ. This scheme has analogous disadvantages and facilitates the acquisition of SL with characteristics akin to the previously described scheme. The scheme presented in Fig. 3, *h*, deviates from the basic one by enabling the addition of auxiliary materials (strengthening, binding, hard-to-pelletize, and structure-forming additives) to the air-charge jet (ACJ). By introducing a relatively small amount (up to 1 – 2 %) of additives, such as an aqueous solution of liquid glass, into the deposited charge, the SL strength can be augmented by 10 – 15 % [4; 5]. The scheme shown in Fig. 3, *i*, incorporates additional measures beyond ACJ pressure. It employs extra strengthening and profiling (height aligning) loads formed by rotating drums mounted on the SL surface before its division. This approach enhances the SL strength and uniformity of its geometric dimensions. However, it entails increased technical complexity and is characterized by enhanced charge buildup on the metal drums.

The scheme illustrated in Fig. 4, *b*, diverges from the basic one due to the inclusion of composite drums. These composite drums account for the differences in the cir-

cumferential velocities of the SL circumferential velocities easing the division of larger diameter SL. Consequently, this modification leads to a 5 % increase in the strength of the nuclei and a reduction in fines content to 33.2 % (Table 2). The scheme displayed in Fig. 4, *c*, uses the pressure from the layer of materials circulating in the pelletizer's working zone, which possesses substantial height and mass. This pressure aids in hardening the SL, facilitating its division upon exiting the lumpy materials layer [4; 5]. This approach results in a 5 – 10 % increase in nuclei strength while maintaining a relatively uniform fractional composition. The pelletizer divider shown in Fig. 4, *d*, employs a curved plow divider with a simplified structure. It enables the generation of nuclei in various sizes, encompassing a significant amount of fines (0 – 2 mm) at 43.4 %, along with larger pellets exceeding 10 mm. The scheme depicted in Fig. 4, *e*, involves a thin metal string stretched across a conical drum, serving as a divider for SL. This innovative design enables the simultaneous division of SL in both longitudinal and transverse directions, requiring significantly less force. It boasts features such as minimal mass buildup, low metal consumption, and high technological effectiveness [4; 5]. Similar devices are utilized in the ceramic industry for mass division before molding. In Fig. 4, *f*, the SL division scheme incorporates a cylindrical drum with wave-shaped ribs acting as a divider to form pelletized nuclei. To counter increased charge buildup, this scheme implements intensive moistening of the drum ribs before SL division, consequently elevating the moisture content of the nuclei. the SL and charge skull profiling schemes depicted in Fig. 4, *g* and *h*, respectively, ensure a constant thickness of the SL, thereby enhancing the uniformity of the fractional composition and resulting in larger average nuclei size A_{nucl} of 6.22 mm. The SL division scheme in Fig. 4, *i*, employs a divider equipped with a system of rods to create a specialized nuclei structure. However, this configuration results in significantly lower strength values compared to those of the basic scheme.

Considering the characteristics of SL and embryonic mass (Θ_M, Θ_S, Θ_W, Table 1, 2) derived from the implemented technical schemes, along with an evaluation of the technological effectiveness of the devices (such as charge buildup, additional equipment material consumption, design complexity, reliability, and operational stability), a combined technological scheme for pellet production is recommended for practical implementation. This recommended scheme encompasses the induced nucleation NSF technology based on SL formation by a single ACJ (Fig. 3, *a*), enabling the utilization of strengthening additives in the deposited charge (Fig. 3, *h*). In this setup, the material is sprayed onto the pre-profiled charge skull (Fig. 4, *g*), and the SL is divided into nuclei using the conical drum equipped with a metal string (Fig. 4, *e*). Implementing the NSF technology based on these components facilitates the production of pellets characterized by reduced moisture content ($\Theta_W = 0.97$), evenly distributed across the cross-section, achieving necessary and sufficient strength ($\Theta_S \geq 1.0$), favorable pore structure, and a maximum yield of pellets sized between 12 to 16 mm ($\Theta_M = 0.72$). These parameters are much lower when conventional nucleation and pelletization technology is used ($\Theta_W = 1.1$, $\Theta_M = 0.33$) [4; 5]. Based on these findings, it is reasonable to anticipate higher pelletizer performance, along with lower energy consumption for thermal drying of pellets during subsequent heat treatment.

Conclusions

The results of studies investigating the performance of technical schemes based on NSF technology, which enables the control of the nucleation and pelletization processes, were analyzed. General principles governing the nucleation and structurization of lumpy mass within this technology framework have been formulated. We assessed the typical variations in parameters Θ_M, Θ_S, Θ_W during the charge formation and pelletization processes for both the basic scheme and several technical schemes under investigation. Through a comprehensive evaluation considering the indicators of NSF technology and technological effectiveness (e.g., charge buildup level, material consumption of additional equipment, design complexity, reliability, and operational stability), specific technical schemes were appraised, and the most efficient solutions were identified. The recommended combined scheme for pellet production utilizes NSF technology based on SL formation by a single air-charge jet (ACJ), permitting the incorporation of strengthening additives. In this approach, the material is sprayed onto a pre-profiled charge skull, and the SL is divided into nuclei using a conical drum equipped with a metal string. Implementing the NSF technology based on these elements allows for the production of pellets characterized by reduced moisture content ($\Theta_W = 0.97$) evenly distributed across the cross-section, achieving necessary and sufficient strength ($\Theta_S \geq 1.0$) and yielding maximum pellets sized between 12 to 16 mm ($\Theta_M = 0.72$). These findings provide grounds to anticipate enhanced pelletizer performance and reduced energy consumption during subsequent pellet heat treatment.

References / Список литературы

1. Pavlovets V.M. *Pellets in Technology of Metals Extraction from Ores*. Moscow, Vologda: Infra-Ingineriya; 2022:284.

Павловец В.М. *Окатыши в технологии экстракции металлов из руд*. Москва, Вологда: Инфра-Инженерия; 2022:284.

2. Abzalov V.M., etc. *Physico-Chemical and Thermal Engineering Fundamentals for Iron Ore Pellets Production*. Ekaterinburg: NPVP "TOREX"; 2012:340.

Абзалов В.М. и др. *Физико-химические и теплотехнические основы производства железорудных окатышей*. Екатеринбург: НПВП «ТОРЕКС»; 2012:340.

3. Yusfin Yu.S., etc. *Production Intensification and Quality Improvement of Pellets*. M.: Metallurgiya; 1994:240.

Юсфин Ю.С. и др. *Интенсификация производства и улучшение качества окатышей*. Москва: Металлургия; 1994:240.

4. Pavlovets V.M. *Expanding the Functionality of Units for Preparing Iron Ore Raw Materials for Metallurgical Smelting*. Moscow, Vologda: Infra-Ingineriya, 2023:328.

Павловец В.М. *Расширение функциональных возможностей агрегатов для подготовки железорудного сырья к металлургической плавке*. Москва, Вологда: Инфра-Инженерия, 2023:328.

5. Pavlovets V.M. *Development of Equipment and Technology for Pelletizing Iron Ore Raw Materials in Metallurgy*. Moscow, Vologda: Infra-Engineering; 2022:336.

Павловец В.М. *Развитие техники и технологии окомкования железорудного сырья в металлургии*. Москва, Вологда: Инфра-Инженерия; 2022:336.

6. Pavlovets V.M. Study of thermal power modes of wet charge spraying intended for induced nucleation. *Izvestiya. Ferrous Metallurgy*. 2009;52(6):9–13.

Павловец В.М. Исследование теплосиловых режимов напыления влажной шихты, предназначенных для принудительного зародышеобразования. *Известия вузов. Черная металлургия*. 2009;52(6):9–13.

7. Iwase K., Higuchi T., Yamamoto T., Murakami T. Design for carbon core pellet toward co-production with sinter. *Tetsu-to-Hagane*. 2021;107(6):483–493. https://doi.org/10.2355/tetsutohagane.TETSU-2020-080

8. Kieush L., Boyko M., Koveria A., Yaholnyk M., Poliakova N. Production of iron ore pellets by utilization of sunflower husks. *Acta Metallurgica Slovaca*. 2021;27(4):167–171. https://doi.org/10.36547/ams.27.4.1052

9. Okeke S.I., Onukwuli O.D. Effect of basicity on metallurgical properties of pellets produced from Itakpe iron ore concentrates. *Discovery and Innovation*. 1999;11(3):170–176. https://doi.org/10.4314/dai.v11i3.15549

10. Frantes K. North American iron mines running flat out to meet domestic and worldwide demand. *Skillings' Mining Review*. 2005;94(7):6–21.

11. *Basics in Mineral Processing*. Metso: Outotec, 2015:752. Available at URL: https://www.metso.com/globalassets/insights/ebooks/mo-basics-in-mineral-processing-handbook_lowres.pdf

12. Goejen J.G., Miller R.A., Brindley W.J., Leissler G.W. *A simulation technique for predicting defects of thermal sprayed coatings: NASA Technical Memorandum TM-106939*, 1995.

13. Hansbo A., Nylén P. Models for the simulation of spray deposition and robot motion optimization in thermal spraying of rotating objects. *Surface and Coatings Technology*. 1999;122(3-4):191–201. https://doi.org/10.1016/S0257-8972(99)00255-8

14. Ensz M.T., Griffith M.L., Reckaway D.E. *Critical issues for functionally graded material deposition by laser engineered net shaping*. Available at URL: http://edge.cs.drexel.edu/GICL/people/schroeder/references/mpif02me.pdf

15. De Los Santos Valladares L., Domínguez A.B., Félix L.L., Kargin J.B., Mukhambetov D.G., Kozlovskiy A.L., Moreno N.O., Santibañez J.F., Cabrera R.C., Barnes C.H.W. Characterization and magnetic properties of hollow α-Fe_2O_3 microspheres obtained by sol gel and spray roasting methods. *Journal of Science: Advanced Materials and Devices*. 2019;4(3):483–491. https://doi.org/10.1016/j.jsamd.2019.07.004

16. Walker W.J., Reed J.S., Verma S.K. Influence of slurry parameters on the characteristics of spray-dried granules. *Journal of the American Ceramic Society*. 1999;82(7):1711–1719.

17. Chen C., Planche M.-P., Deng S., Huang R., Ren Z., Liao H. Strengthened peening effect on metallurgical bonding formation in cold spray additive manufacturing. *Journal of Thermal Spray Technology*. 2019;28:769–779. https://doi.org/10.1007/s11666-019-00854-4

18. Assadi H., Gartner F., Stoltenhoff T., Kreye H. Bonding mechanism in cold gas spraying. *Acta Materialia*. 2003;51(15):4379–4394. https://doi.org/10.1016/S1359-6454(03)00274-X

19. Dorfman M. Thermal spray materials. *AM&P Technical Articles*. 2002;160:49–51.

20. Kasparova M., Houdkova S., Cubrova J. Thermally sprayed coatings for high temperature application. In: *Proceedings of the 21st Int. Conf. on Metallurgy and Materials, Brno, Czech Republic, 23–25.05.2012*. 2012:144–146.

Information about the Author / Сведения об авторе

Viktor M. Pavlovets, *Cand. Sci. (Eng.), Assist. Prof. of the Chair "Thermal Power and Ecology",* Siberian State Industrial University
E-mail: pawlowets.victor@yandex.ru

Виктор Михайлович Павловец, *к.т.н., доцент кафедры теплоэнергетики и экологии,* Сибирский государственный индустриальный университет
E-mail: pawlowets.victor@yandex.ru

Received 11.05.2022
Revised 16.11.2022
Accepted 04.09.2023

Поступила в редакцию 11.05.2022
После доработки 16.11.2022
Принята к публикации 04.09.2023